Efficient Pathway to Neutralization of Multiply Charged Ions Produced in Auger Processes

V. Stumpf,[1] P. Kolorenč,[2] K. Gokhberg,[1,*] and L. S. Cederbaum[1]

[1]*Theoretische Chemie, Physikalisch-Chemisches Institut, Universität Heidelberg, Im Neuenheimer Feld 229, D-69120 Heidelberg, Germany*

[2]*Charles University in Prague, Faculty of Mathematics and Physics, Institute of Theoretical Physics, V Holešovičkách 2, 180 00, Prague, Czech Republic*

(Received 7 March 2013; published 21 June 2013)

After core ionization of an atom or molecule by an x-ray photon, multiply charged ions are produced in the Auger decay process. These ions tend to neutralize their charge when embedded in an environment. We demonstrate that, depending on the atom or molecule and its neighbors, electron transfer mediated decay (ETMD) provides a particularly efficient neutralization pathway for the majority of the ions produced by Auger decay. The mechanism is rather general. As a showcase example, we conducted an *ab initio* study of the $NeKr_2$ cluster after core ionization of the Ne atom. This example has been chosen because it is amenable to both *ab initio* calculations and coincidence experiments. We find that even for frozen nuclei, the neutralization rate can be as fast as 0.130 ps^{-1}. We also show that nuclear dynamics may increase the rate by about an order of magnitude. The generality of the mechanism makes this neutralization pathway important in weakly bonded environments.

DOI: 10.1103/PhysRevLett.110.258302 PACS numbers: 82.33.Fg, 32.80.Hd, 36.40.Wa, 82.50.Kx

Interaction of an x-ray photon with an atom leads to the efficient ionization of atomic core electrons, if the photon energy lies above the corresponding ionization threshold. Ionization cross sections of electrons from valence shells at the energies in question are usually orders of magnitude smaller than the cross sections for core ionization [1]. Therefore, it is mostly highly excited ions with a core vacancy that are produced in x-ray photon absorption. For not too heavy atoms, such ions decay on a femtosecond time scale via the nonradiative Auger process [2]. One or several secondary Auger electrons can be emitted in this decay leading to the production of multiply-charged ions with vacancies in the valence shell [2]. Both core ionization and Auger decay remain essentially atomic processes in weakly bound systems. Thus, following the Auger decay one usually obtains multiple charge localized at the site where the initial core vacancy resided [3,4].

What happens to the multiply charged ions produced in the Auger process? For transparency of discussion, we concentrate here on the ions produced in the decay of not too deep core levels to exclude Auger cascades, where several successive Auger decays take place [5,6]. In an isolated system the excited multiply charged ions produced will decay slowly by photon emission typically in the range of seconds to 0.1 ns [7]. On the other hand, in the presence of neighbors the energy of the multiply charged ion may be considerable relative to the energy of the neighbors and interatomic or intermolecular processes may take place. If the excess electronic energy of the ion suffices to ionize a neighbor, it has been shown that interatomic Coulombic decay in which the ion relaxes and its excess energy is used to ionize a neighbor is the dominant relaxation mechanism [8–10]. This ultrafast process, which typically proceeds within 1–100 fs [11,12], does not change the charge of the ion. For the less highly excited ions, it is usually assumed that neutralization of the ion will take place [13]. This process is known to proceed by electron transfer from a neighboring species. If the potential surfaces of the ionic and the charge transfer states cross, then charge transfer may take place when the nuclear configuration corresponds to the crossing point [14,15]. If no suitable crossing exists, charge transfer may proceed radiatively, typically on a nanosecond scale, and is accompanied by the photon emission (radiative charge transfer) [16,17]. In the latter process the energy released upon neutralization of the ion is transferred to the electromagnetic field, while in the former one it is converted into the kinetic energy of the nuclei.

Interestingly, the majority of ions produced in Auger decay do not possess enough excess electronic energy to undergo interatomic Coulombic decay [8]. We show here that electron transfer mediated decay (ETMD) is a highly efficient general pathway for neutralization of exactly these low-excited multiply charged ions produced in the Auger process. In ETMD (see Fig. 1) a neighbor donates an electron to the ion, while the released energy is simultaneously transferred either to the donor or to another neighboring species ionizing an additional electron [18–20]. Therefore, the neutralization of ions via ETMD is accompanied by an increase in the charge state of the complete system. To distinguish the processes involving two or three species, they are denoted as ETMD(2) and ETMD(3), respectively.

The final states of ETMD lie in the electronic continuum and, therefore, the resonant condition is fulfilled for all nuclear configurations at which this channel is energetically open. Consequently, no nuclear motion is necessary to enable the neutralization via ETMD in sharp contrast to

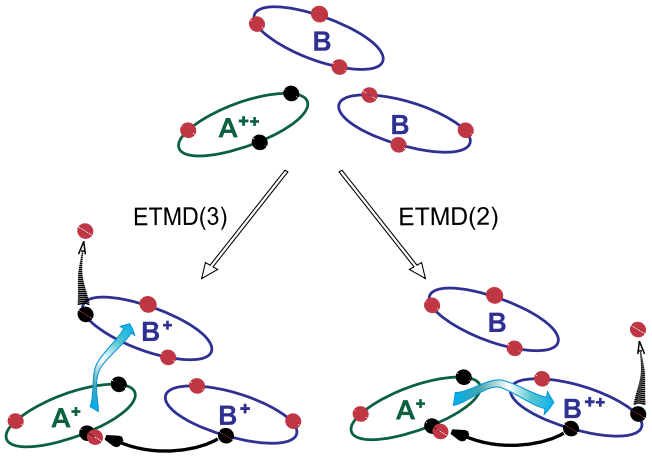

FIG. 1 (color online). Schematic description of the ETMD process for the dication A^{++} produced by Auger decay following core ionization of A. An electron is donated by a neighboring atom B (solid black arrow) and fills a vacancy on the dication A^{++}. Simultaneously, the excess energy (blue arrow) is transferred either to the donor [ETMD(2) pathway] or to a different neighbor [ETMD(3) pathway] ionizing it. Coulomb explosion follows the ETMD step. Note the different distribution of positive charge resulting in the ETMD(3) and ETMD(2) processes.

the charge transfer via potential crossing. The nuclei do not have to reach the crossing point which consumes time, and, being in the electronic continuum, the potential surfaces of the ionic and the charge transfer states are separated energetically and typically do not cross for the situations discussed here. Moreover, the decay mechanism of ETMD is given by electron-electron interaction [18], which for the energies involved is usually much stronger than the coupling to the electromagnetic field. This all results in ETMD rates being much larger than those of charge transfer by curve crossing and radiative charge transfer.

To be specific, we study the neutralization of ions following Auger decay in the rare gas $NeKr_2$ trimer. We have chosen this showcase example because it is amenable to both *ab initio* calculations and coincidence experiments. In the Auger decay of the $1s$ vacancy of isolated Ne, the majority of the final ionic states have two holes in the outer-valence $2p$ electronic shell [21]. These comprise the excited states, $Ne^{++}(2p^{-2}\,{}^1D)$ (61% Auger yield) and $Ne^{++}(2p^{-2}\,{}^1S)$ (10% Auger yield), and the dicationic ground state $Ne^{++}(2p^{-2}\,{}^3P)$ (very small Auger yield). The former states lie only a few eV above the latter one and decay slowly by photon emission. In the $NeKr_2$ cluster the bonding between the Ne and Kr atoms is very weak and the Auger decay occurs locally on the Ne atom, and we may assume that the populations of the states correlating with $Ne^{++}(2p^{-2}\,{}^1D, {}^1S)$ do not deviate appreciably from the atomic values. The relaxation of the ions via ETMD is, however, fast in the cluster as we will see below. According to our calculations, at the equilibrium geometry of the cluster only ETMD(3) is energetically allowed for $Ne^{++}(2p^{-2}\,{}^1D)$, whereas for the higher lying ${}^1S$ state also a few ETMD(2) channels are open. We find that the ETMD(3) mode plays the major role in this particular example and, therefore, we will concentrate on this mode below. Auger decay followed by ETMD(3) is summarized in the following two-step scheme (see also Fig. 1 for the last step):

$$\begin{aligned} Ne^+(1s^{-1})Kr_2 &\rightarrow Ne^{++}(2p^{-2}\,{}^1D, {}^1S)Kr_2 + e_{\text{Auger}} \\ Ne^{++}(2p^{-2})Kr_2 &\rightarrow Ne^+(2p^{-1})(Kr^+(4p^{-1}))_2 + e_{\text{ETMD}} \\ &\rightarrow Kr^+ + Ne^+ + Kr^+. \end{aligned}$$

In this ETMD pathway a slow electron with characteristic energy and three singly charged ions are produced. The last step in the scheme stands for the resulting Coulomb explosion after ETMD. Detecting electrons and ions in coincidence and determining their energies, as is done for example in the COLTRIMS (cold target recoil ion momentum spectroscopy) technique [22], allows the unambiguous experimental identification of this process as has been done in other cases [23–25].

The Auger lifetime of the $1s$ vacancy in Ne is about 4.4 fs [21] and is much shorter than the characteristic vibrational frequencies in the neutral $NeKr_2$ cluster. Therefore, the Auger decay proceeds essentially at the equilibrium geometry of the ground state of this system. We first discuss the ETMD channels and the corresponding rates at this geometry. The effect of nuclear dynamics on the ETMD process will be considered later on.

To study the ETMD one needs the potential surfaces and decay rates as input data. First, the equilibrium geometry of the neutral $NeKr_2$ cluster was determined by means of the coupled cluster method, including singles, doubles, and perturbative triples [CCSD(T)] as implemented in the MOLPRO quantum chemistry package [26,27]. For both Ne and Kr aug-cc-pVQZ correlation consistent basis sets [28,29] located on the corresponding atoms were used. Three sets of additional $3s3p2d2f1g$ midbond basis functions were used between the pairs of atoms [30]. The optimized geometry of $NeKr_2$ has a C_{2v} symmetry with Ne-Kr interatomic distance $r = 3.68$ Å and KrNeKr angle $\theta = 67.01°$ (see Fig. 2).

The energies of the $Ne^{++}(2p^{-2}\,{}^1D)Kr_2$ electronic states decaying by ETMD were determined using the *ab initio* algebraic diagrammatic construction scheme for the two-particle propagator [ADC(2)] [31–33]. The aug-cc-pVQZ basis sets located on the Ne and Kr atoms were used in this calculation. The restricted Hartree-Fock orbitals and integrals needed as input data for ADC(2) were generated by a self-consistent field routine implemented in the MOLCAS quantum chemistry package [34]. The five $Ne^{++}(2p^{-2}\,{}^1D)Kr_2$ states, being degenerate at infinite Ne-Kr distances, split only weakly at the equilibrium geometry of $NeKr_2$ and lie in the energy range of 65.07–65.09 eV. The single $Ne^{++}(2p^{-2}\,{}^1S)Kr_2$ state is at 68.76 eV. The energies of the final states

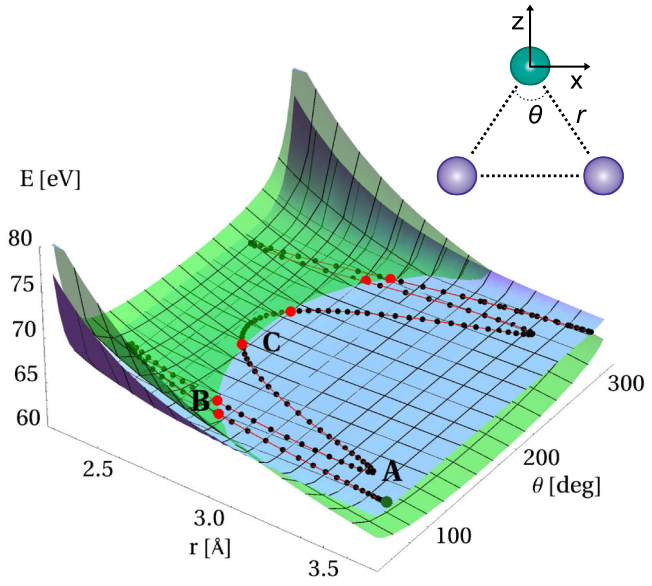

FIG. 2 (color online). Potential energy surfaces of the decaying $Ne^{++}(2p^{-2}\,{}^1D)Kr_2$ b_1 state and of the ETMD(3) final state $Ne^{+}(2p^{-1})(Kr^{+}(4p^{-1}))_2$. The classical trajectory starts at the equilibrium geometry of the neutral cluster (point A) and is plotted on the PES of the decaying state. The two surfaces cross each other and where the final state is higher in energy than the state populated by the Auger process, the ETMD is prohibited. Red dots, like points B and C, denote the positions of ETMD(3) thresholds along the trajectory.

$Ne^{+}(2p^{-1})(Kr^{+}(4p^{-1}))_2$ of ETMD(3) were calculated by adding to the ground state potential energy of $NeKr_2$ the triple ionization potential approximated analytically as $IP(\mathrm{Ne}) + 2IP(\mathrm{Kr}) + 2/R_{\mathrm{NeKr}} + 1/R_{\mathrm{KrKr}}$. The abbreviation $IP(X)$ stands for the ionization potential of atom X, and R_{XY} is the distance between atoms X and Y. At the equilibrium geometry of the neutral cluster, the energy of the ETMD(3) final states is 61.81 eV.

The ETMD rates cannot be computed by commercial program packages. These rates were obtained employing the Fano-ADC-Stieltjes approach [35], which relies on the Fano ansatz to represent electronic resonances. We used the cc-pVTZ basis set augmented by $4s4p4d$ for Ne and the cc-pVTZ basis set augmented by $5s5p5d$ Kaufmann-Baumeister-Jungen [36] continuumlike basis functions for Kr. The values of ETMD rates for the five $Ne^{++}(2p^{-2}\,{}^1D)Kr_2$ states lie in the range of 0.031–0.130 ps^{-1}, and that for the $Ne^{++}(2p^{-2}\,{}^1S)Kr_2$ state is 0.029 ps^{-1}. Since electron transfer takes place in ETMD, its rate depends strongly on the orbital overlap between the charge donor and the doubly ionized unit [18]. The values of the ETMD rates for individual $Ne^{++}(2p^{-2}\,{}^1D)Kr_2$ states reflect the varying efficiency of the orbital overlap between Ne^{++} and Kr arising from the different spatial orientation of the orbitals where the holes are located. The highest decay rate of 0.13 ps^{-1} is observed for the state of b_1 symmetry, where the leading two-hole configuration is of $2p_x^{-1}2p_z^{-1}$ character and both orbitals with holes lie in the plane of the trimer. Conversely, the state of a_1 symmetry, where the leading two-hole configuration has out-of-plane $2p_y^{-2}$ character, shows the lowest decay rate (0.031 ps^{-1}). One can see that ETMD, occurring on the picosecond time scale, is a relatively fast decay mode for the $Ne^{++}(2p^{-2})Kr_2$ states already at the fixed equilibrium geometry of the $NeKr_2$ cluster.

The dependence on orbital overlap leads to an exponential increase of the ETMD rate with decreasing distance between the electron donor (Kr) and the acceptor (Ne). Therefore, the question arises, what impact will the nuclear dynamics have on the decay efficiency? To estimate this impact, we computed the potential energy surface (PES) of the $Ne^{++}(2p^{-2}\,{}^1D)Kr_2$ b_1 state (see Fig. 2). The equilibrium geometry in this state is linear and possesses $D_{\infty h}$ symmetry with a Ne-Kr internuclear distance of 2.7 Å. One may assume that the nuclear dynamics in this decaying state will preserve the symmetry; i.e., the symmetric stretching and the bending modes are the relevant modes. To reduce the computational effort we, thus, considered only coordinates preserving the C_2v symmetry (r and θ).

On the PES of the b_1 state we computed the classical trajectory for the first 650 femtoseconds of the decay, starting from the equilibrium geometry of the neutral cluster (see Fig. 2). We also calculated the ETMD rates along the resulting trajectory (see Fig. 3). The ETMD(3) channel is open only in the region where the tricationic $Ne^{+}(2p^{-1})(Kr^{+}(4p^{-1}))_2$ final states are lower in energy than the decaying b_1 state. After the Auger process, the attractive interaction between the Ne^{++} ion and the Kr atoms leads initially to a shortening of the Ne-Kr distances (see trajectory between A and B in Fig. 2) followed by a fast oscillation in the symmetric stretch mode. As can be seen from Fig. 3, the ETMD rate increases steeply as the Ne-Kr distance decreases, until the channel becomes closed at the threshold marked B in Fig. 2. The bending mode becomes active between 215 and 315 fs, leading to an increase in the angle θ. The simultaneous increase of the Kr-Kr distance lowers the energy of the final state allowing the ETMD channel to remain open for Ne-Kr distances to within 2.7 Å (the ETMD threshold marked C). Close to this interatomic distance the ETMD rate increases nearly 100-fold reaching the value 11.5 ps^{-1}. Therefore, one can see that the decay is at its fastest for nuclear configurations close to the linear Kr-Ne-Kr geometry.

We computed the ETMD yield $P(t)$ along the trajectory by using the semiclassical formula $P(t) = (1 - e^{-\int_0^t \Gamma(t')dt'})$ where $\Gamma(t')$ is the computed ETMD rate along the trajectory (see Fig. 3). After 650 fs about 50% of the initial b_1 state population has decayed via ETMD, which corresponds to an average lifetime of approximately 1 ps (average ETMD rate: 1 ps^{-1}). The nuclear dynamics initiated by a sudden double ionization of the Ne atom via the Auger process leads to an almost tenfold increase of the neutralization rate compared to that obtained at the frozen equilibrium

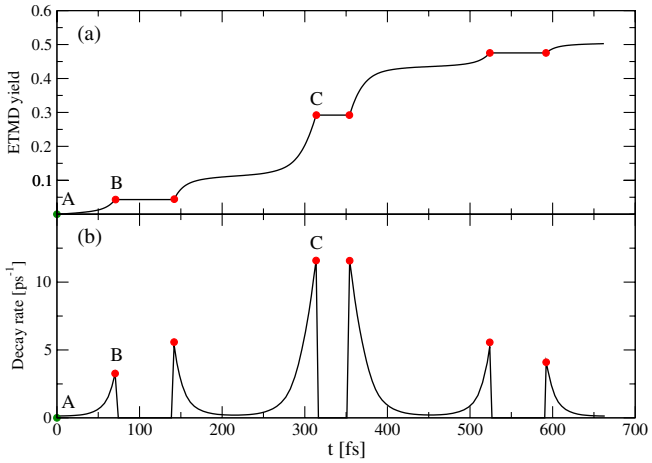

FIG. 3 (color online). Effect of nuclear dynamics on the ETMD(3) process in $Ne^{++}Kr_2$ cluster. Lower panel: the ETMD(3) rate along the trajectory given in Fig. 2. Note the rapid exponential increase in the rate with the decreasing Ne-Kr distance (e.g section *A*–*B*). The maximum rate achieved along the trajectory (point *C*) is 11.5 ps^{-1} and is about ninety times larger than the rate at the initial nuclear configuration (geometry of the neutral ground state). Upper panel: the ETMD yield accumulated along the trajectory. The majority of the decay events takes place between 210 and 450 fs at nuclear configurations close to the $D_{\infty h}$ Kr-Ne-Kr geometry.

geometry (0.13 ps^{-1}). This increase is due to the appearance of an attractive potential after the Auger process leading to the shortening of the interatomic distances between the ion and the neutrals. This conclusion should remain valid for the ETMD driven neutralization of ions following Auger decay in general polarizable environments.

We demonstrated that the doubly ionized Ne species which are produced by Auger decay in $NeKr_2$ cluster are efficiently neutralized via the ETMD process. The neutralization takes place on the time scale of a few picoseconds already at the fixed equilibrium geometry of the neutral cluster, and is orders of magnitude faster than the competing radiative charge transfer. No crossing of the potential surfaces of the ionic and of charge transfer states were found. We stress further that the ETMD rates increase with the number N of nearest neighbors, which is an expected situation when a multiply charged ion is created in a medium. Indeed, the ETMD(2) rate depends linearly on N, while ETMD(3) rate grows as $N(N-1)/2$. In a system where the Ne^{++} ion has 6 Kr neighbors at similar distances, the latter rate will grow 15-fold, and the neutralization will proceed on the femtosecond scale. We have also seen that the ETMD rates depend strongly on the orbital overlap between the ionized moiety and the neighboring species and grow exponentially as the distance between the two decreases. Therefore, one can expect faster neutralization of ions in hydrogen bonded systems than in the van der Waals clusters considered in this Letter. First hints for that have been reported [37].

We would also like to stress that the neutralization of ions via ETMD is not limited to doubly ionized species but is rather a general mechanism operative for ions in an arbitrary ionization state. Such ions may be obtained, for example, in the electron shakeoff process or if more than one electron is emitted in the Auger decay (double Auger process) [38]. Indeed, the ETMD(2) process of triply ionized Ar has been recently observed following Auger decay in Ar dimers [20]. Alternatively, multiply charged ions may be produced after Auger decay of cationic species. Potentially interesting systems to study ETMD driven neutralization following Auger process are the hydrated ions of alkali and alkaline-earth metals.

In biological medium the neutralization of ions following Auger decay was shown experimentally to be an important factor in causing damage to cellular DNA [39]. In such settings we may speculate that ETMD might be an important neutralization pathway. Here, one may expect its rates to be considerably higher than in the model system presented in this work allowing ETMD to efficiently compete with other possible charge transfer processes. The following characteristics of the ETMD process could play a role in understanding the enhanced cytotoxic effects of charge neutralization. First, ETMD is accompanied by the production of a slow electron having energy of several eV. The attachment of electrons in the 4 to 20 eV range to DNA was shown to be particularly effective in causing DNA strand breaks [40,41]. Second, ionization of neighbors in ETMD leads to the production of radical species. For example, the ETMD(3) process involving the ionization of two water molecules in the DNA solvation shell could result in the production of two OH radicals extremely active in causing the so-called indirect damage to the DNA strands [42]. We hope that studying the ETMD driven charge neutralization in biological settings will provide further understanding of the causes of DNA damage.

Finally, we mention that the neutralization of slow ions on surfaces has attracted much attention (see the review [43] and references therein). Many studies are done on metallic surfaces, where the surface as a whole transfers a charge to the incoming ion and emits an electron to the vacuum to compensate for the excess energy. Our present findings suggest to also study the neutralization of slow ions on layers of organic molecules adsorbed on surfaces where a molecular picture similar to that discussed here for ETMD is expected to be applicable.

In conclusion, we showed in this Letter that electron transfer mediated decay provides a pathway for multiply charged ions produced in Auger decay to be efficiently neutralized by their neighbors. If the ETMD channel is energetically open, the majority of the ions produced by Auger will undergo ETMD. In contrast to other, more common charge transfer processes, ETMD occurs even at frozen nuclear configurations. Explicit *ab initio* calculations on the $NeKr_2$ cluster show that already at the equilibrium geometry

of this cluster the neutralization of Ne^{++} ions occurs between 8 and 30 ps. It was also estimated that the nuclear dynamics tend to increase the neutralization rates by up to an order of magnitude. The computed rates suggest that ETMD should efficiently compete with radiative and nonradiative charge transfer processes. The proposed mechanism is general and may accompany Auger decay of atoms and molecules in weakly bonded environments. Here, it is important that the ETMD rates increase substantially with the number of neighbors making ETMD a dominant mechanism. Since Auger processes are known to accompany the absorption of high-energy radiation by biological media, further studies of the proposed neutralization mechanism may shed light on the origin of damages in cells.

The authors thank Y.-C. Chiang for the generous help with calculations. The research leading to these results has received funding from the European Research Council under the European Community's Seventh Framework Programme (FP7/2007-2013)/ERC Advanced Investigator Grant No. 227597. P. K. acknowledges financial support from the Czech Science Foundation (Project No. GAČR P208/12/0521).

*kirill.gokhberg@pci.uni-heidelberg.de

[1] J. Yeh and I. Lindau, At. Data Nucl. Data Tables **32**, 1 (1985).
[2] W. Bambynek, B. Crasemann, R. W. Fink, H. U. Freund, H. Mark, C. D. Swift, R. E. Price, and P. V. Rao, Rev. Mod. Phys. **44**, 716 (1972).
[3] M. Lundwall, M. Tchaplyguine, G. Öhrwall, A. Lindblad, S. Peredkov, T. Rander, S. Svensson, and O. Björneholm, Surf. Sci. **594**, 12 (2005).
[4] W. Pokapanich, N. V. Kryzhevoi, N. Ottosson, S. Svensson, L. S. Cederbaum, G. Öhrwall, and O. Björneholm, J. Am. Chem. Soc. **133**, 13430 (2011).
[5] T. A. Carlson and M. O. Krause, Phys. Rev. **137**, A1655 (1965).
[6] M. O. Krause and T. A. Carlson, Phys. Rev. **158**, 18 (1967).
[7] Y. Ralchenko, A. E. Kramida, J. Reader, and NIST ASD Team, NIST Atomic Spectra Database (version5.0) online, http://physics.nist.gov/asd (2012).
[8] R. Santra and L. S. Cederbaum, Phys. Rev. Lett. **90**, 153401 (2003).
[9] Y. Morishita, X.-J. Liu, N. Saito, T. Lischke, M. Kato, G. Prümper, M. Oura, H. Yamaoka, Y. Tamenori, I. H. Suzuki *et al.*, Phys. Rev. Lett. **96**, 243402 (2006).
[10] K. Kreidi, T. Jahnke, T. Weber, T. Havermeier, X. Liu, Y. Morisita, S. Schössler, L. Schmidt, M. Schöffler, M. Odenweller *et al.*, Phys. Rev. A **78**, 043422 (2008).
[11] U. Hergenhahn, J. Electron Spectrosc. Relat. Phenom. **184**, 78 (2011).
[12] V. Averbukh, P. V. Demekhin, P. Kolorenč, S. Scheit, S. D. Stoychev, A. I. Kuleff, Y.-C. Chiang, K. Gokhberg, S. Kopelke, N. Sisourat *et al.*, J. Electron Spectrosc. Relat. Phenom. **183**, 36 (2011).
[13] By neutralization we mean that at least one of the ion's charges is compensated by an electron provided by the environment.
[14] R. A. Marcus, Rev. Mod. Phys. **65**, 599 (1993).
[15] M. D. Newton and N. Sutin, Annu. Rev. Phys. Chem. **35**, 437 (1984).
[16] N. Saito, Y. Morishita, I. Suzuki, S. Stoychev, A. Kuleff, L. Cederbaum, X.-J. Liu, H. Fukuzawa, G. Prümper, and K. Ueda, Chem. Phys. Lett. **441**, 16 (2007).
[17] L. B. Zhao, J. G. Wang, P. C. Stancil, J. P. Gu, H.-P. Liebermann, R. J. Buenker, and M. Kimura, J. Phys. B **39**, 5151 (2006).
[18] J. Zobeley, R. Santra, and L. S. Cederbaum, J. Chem. Phys. **115**, 5076 (2001).
[19] M. Förstel, M. Mucke, T. Arion, A. M. Bradshaw, and U. Hergenhahn, Phys. Rev. Lett. **106**, 033402 (2011).
[20] K. Sakai, S. Stoychev, T. Ouchi, I. Higuchi, M. Schöffler, T. Mazza, H. Fukuzawa, K. Nagaya, M. Yao, Y. Tamenori *et al.*, Phys. Rev. Lett. **106**, 033401 (2011).
[21] H. P. Kelly, Phys. Rev. A **11**, 556 (1975).
[22] A. Czasch, L. Schmidt, T. Jahnke, T. Weber, O. Jagutzki, S. Schössler, M. S. Schöffler, R. Dörner, and H. Schmidt-Böcking, Phys. Lett. A **347**, 95 (2005).
[23] T. Jahnke, A. Czasch, M. Schöffler, S. Schössler, A. Knapp, M. Käsz, J. Titze, C. Wimmer, K. Kreidi, R. Grisenti *et al.*, Phys. Rev. Lett. **93**, 163401 (2004).
[24] N. Sisourat, N. V. Kryzhevoi, P. Kolorenč, S. Scheit, T. Jahnke, and L. S. Cederbaum, Nat. Phys. **6**, 508 (2010).
[25] N. Sisourat, H. Sann, N. V. Kryzhevoi, P. Kolorenč, T. Havermeier, F. Sturm, T. Jahnke, H.-K. Kim, R. Dörner, and L. S. Cederbaum, Phys. Rev. Lett. **105**, 173401 (2010).
[26] H.-J. Werner, P. J. Knowles, G. Knizia, F. R. Manby, and M. Schütz, Wiley Interdiscip. Rev.: Comput. Mol. Sci. **2**, 242 (2012).
[27] H.-J. Werner *et al.*, MOLPRO, version 2012.1, a package of *ab initio* programs (2012), see http://www.molpro.net.
[28] J. T. H. Dunning, J. Chem. Phys. **90**, 1007 (1989).
[29] A. Wilson, D. Woon, K. Peterson, and J. T. H. Dunning, J. Chem. Phys. **110**, 7667 (1999).
[30] S. M. Cybulski and R. R. Toczylowski, J. Chem. Phys. **111**, 10520 (1999).
[31] J. Schirmer and A. Barth, Z. Phys. A **317**, 267 (1984).
[32] F. Tarantelli, L. Cederbaum, and A. Sgamellotti, J. Electron Spectrosc. Relat. Phenom. **76**, 47 (1995).
[33] F. Tarantelli, Chem. Phys. **329**, 11 (2006).
[34] F. Aquilante, L. De Vico, N. Ferré, G. Ghigo, P.-A. Malmqvist, P. Neogrády, T. B. Pedersen, M. Pitonak, M. Reiher, B. O. Roos *et al.*, J. Comput. Chem. **31**, 224 (2010).
[35] P. Kolorenč, V. Averbukh, K. Gokhberg, and L. S. Cederbaum, J. Chem. Phys. **129**, 244102 (2008).
[36] K. Kaufmann, W. Baumeister, and M. Jungen, J. Phys. B **22**, 2223 (1989).
[37] I. B. Müller and L. S. Cederbaum, J. Chem. Phys. **122**, 094305 (2005).
[38] T. A. Carlson and M. O. Krause, Phys. Rev. Lett. **14**, 390 (1965).
[39] P. N. Lobachevsky and R. F. Martin, Radiat. Res. **153**, 271 (2000).
[40] B. Boudaïffa, P. Cloutier, D. Hunting, M. A. Huels, and L. Sanche, Science **287**, 1658 (2000).
[41] E. Alizadeh and L. Sanche, Chem. Rev. **112**, 5578 (2012).
[42] P. O'Neill, in *Radiation Chemistry: Present Status and Future Trends*, edited by C. D. Jonah and B. S. M. Rao (Elsevier Science B.V., Amsterdam, 2001).
[43] H. Brongersma, M. Draxler, M. de Ridder, and P. Bauer, Surf. Sci. Rep. **62**, 63 (2007).